Results in Chemistry 7 (2024) 101415

Contents lists available at ScienceDirect

Results in Chemistry

journal homepage: www.sciencedirect.com/journal/results-in-chemistry

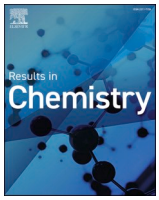

# Concentration-dependence of specific rotation of optically active glycerol analogues and structurally related compounds: The significance of intermolecular hydrogen bonding

Michiyasu Nakao, Akihito Nakamura, Shoki Yamada, Syuji Kitaike, Shigeki Sano *

*Graduate School of Pharmaceutical Sciences, Tokushima University, Sho-machi, Tokushima 770-8505, Japan*

ARTICLE INFO

*Keywords:*
Glycerol
Intermolecular hydrogen bonding
Concentration dependence
Specific rotation
$^1$H NMR spectroscopy
X-ray crystallography

ABSTRACT

Specific rotation of optically active glycerol analogues, (*S*)-3-(benzyloxy)propane-1,2-diol [(*S*)-**1**], (*S*)-3-methoxypropane-1,2-diol [(*S*)-**6**] and (*S*)-3-phenoxypropane-1,2-diol [(*S*)-**13**], changed its sign from (+) to (–) with increasing concentration in $CHCl_3$, whereas no significant concentration-dependent change was observed in MeOH. The $^1$H NMR spectrum of (*S*)-**1** showed concentration-dependent changes of the chemical shift in $CDCl_3$. Intermolecular interaction by OH···OH hydrogen bonds was suggested by single crystal X-ray crystallography of (*S*)-**13**. The concentration-dependent changes of specific rotation of (*S*)-**1**, (*S*)-**6**, and (*S*)-**13** in $CHCl_3$ can therefore be presumed to be due to self-assembly of these compounds via intermolecular hydrogen bonding at high concentration. The remarkable concentration-dependent changes in specific rotation were also observed to occur in the compounds with related chemical structures, such as (*S*)-3-hydroxy-4-methoxy-4-oxobutanoic acid [(*S*)-**10**], (*S*)-1-[(2-methylpropan-2-yl)oxycarbonyl]pyrrolidine-2-carboxylic acid [Boc-L-Pro-OH, (*S*)-**14**], (*R*)-3-hydroxy-4,4-dimethylhydrofran-2(3*H*)-one [(*R*)-**15**], (*R*)-tetrahydrofuran-2-carboxylic acid [(*R*)-**16**], (*S*)-3-methyl-2-[(2-methylpropan-2-yl)oxycarbonylamino]butanoic acid [Boc-L-Val-OH, (*S*)-**17**], (*R*)-oxiran-2-ylmethanol [(*R*)-**18**], and (4*S*)-4-isopropyloxazolidin-2-one [(*S*)-**19**]. The existence of intermolecular interaction by C=O···HO hydrogen bonds was suggested by single crystal X-ray crystallography of (*S*)-**10**, (*S*)-**13**, and (*S*)-**14**. Thus, this series of chiral compounds have multiple functional groups in appropriate positions that serve as hydrogen-bond donors and/or acceptors, resulting in significant concentration-dependent changes of specific rotation.

## 1. Introduction

The specific rotation [$\alpha$] of a chiral compound is defined based on the observed optical rotation under the standard conditions, namely the concentration (1 g/mL) and the path length (1 dm). However, it is difficult to use the standard conditions all the time, and thus the specific rotation is calculated from the observed rotation α in degree via the following Eq. (1), where [$\alpha$] is the specific rotation, $\alpha$ is the observed rotation, $l$ is the path length (dm), and $c$ is the concentration (g/dL) [1–5].

$$[\alpha] = \frac{100\alpha}{l \times c} \quad (1)$$

The specific rotation is influenced by measurement temperature, wavelength of light employed, and solvent, but when the same temperature, the same wavelength, and the same solvent are used, it is regarded as a physical constant of a chiral compound in the same manner as its melting point, boiling point, and density. Previously, we reported the synthetic method of glycerophospholipids using Horner-Wadsworth-Emmons reaction of mixed phosphonoacetate [6,7]. At that time, (*S*)-3-(benzyloxy)propane-1,2-diol [(*S*)-**1**], the optically active intermediate of the synthetic pathway, showed different specific rotations depending on the measurement concentration of (*S*)-**1** (Fig. 1). It has been reported in the literature that the specific rotation values of (*S*)- and (*R*)-**1** differ depending on the measurement conditions. For example, (*S*)-**1** was reported to have specific rotation of $[\alpha]_D^{20}$ –5.4 (pure) [8], $[\alpha]_D^{23}$ –3.64 (*c* 6.59, $CHCl_3$) [9], $[\alpha]_D^{20}$ + 2.50 (*c* 1.0, $CHCl_3$: 90 % ee) [10], and $[\alpha]_D^{20}$ –5.48 (*c* 20, $CHCl_3$) [11], while (*R*)-**1** was reported to have specific rotation of $[\alpha]_D^{21}$ –0.98 (*c* 1.02, $CHCl_3$: 73 % ee) [12], $[\alpha]_D^{20}$ + 4.7 (*c* 1.0, $CHCl_3$) [13], $[\alpha]_D^{25}$ + 5.5 (*c* 10, $CHCl_3$) [14], $[\alpha]_D^{20}$ + 4.7 (*c*

* Corresponding author.
*E-mail address:* ssano@tokushima-u.ac.jp (S. Sano).

https://doi.org/10.1016/j.rechem.2024.101415
Received 21 February 2024; Accepted 1 March 2024
Available online 2 March 2024

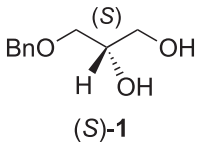


(*S*)-**1**

**Fig. 1.** Chemical structure of (*S*)-3-(benzyloxy)propane-1,2-diol [(*S*)-**1**].

4.7, $CHCl_3$) [15], $[\alpha]_D^{22}$ + 5.63 (*c* 20, $CHCl_3$) [16], and $[\alpha]_D^{20}$ + 5.9 (*c* 1, $CHCl_3$) [17]. In the product specification tables of Sigma-Aldrich, the specific rotation is described as $[\alpha]_D^{20}$ –4.7 (*c* 20, $CHCl_3$) for (*S*)-**1** and $[\alpha]_D^{20}$ + 5.5 (*c* 20, $CHCl_3$) for (*R*)-**1**. It has been known for decades that L-malic acid [(*S*)-**2**] changes its specific rotation even in sign with change in its concentration in water, but the detailed reasons for this change are unclear [18,19]. Herein, we report the remarkable concentration-dependent changes in the specific rotation of (*S*)-**1** and its structurally related compounds, together with the data of $^1$H NMR spectroscopy and X-ray crystallography.

## 2. Experimental section

All melting points were determined on a Yanagimoto micro melting point apparatus and are uncorrected. IR spectra were obtained with a JASCO FT/IR-6200 IR Fourier transform spectrometer. $^1$H NMR (500 MHz) and $^{13}$C NMR (125 MHz) spectra were recorded with a Bruker AV500 spectrometer. Chemical shifts are given in δ values (ppm) using TMS as an internal standard. All reactions were monitored by TLC employing 0.25 mm silica gel plates (Merck 5715; 60 $F_{254}$). HRMS (ESI) data were recorded with a Waters LCT Premier spectrometer. Elemental combustion analyses were performed with a J-SCIENCE LAB JM10. Column chromatography was carried out on silica gel [Silica Gel PSQ 60B (Fuji Silysia Chemical)]. Anhydrous THF, $CH_2Cl_2$, MeOH and DMF were used as purchased from Kanto Chemical. All other reagents including (*R*)-**3**, (*S*)-**13**, (*S*)-**14**, (*R*)-**15**, (*R*)-**16**, (*S*)-**17**, (*R*)-**18**, and (*S*)-**19** were used as purchased. Specific rotations were recorded on JASCO digital polarimeter P-2200 using a cylindrical glass cell (3.5 mm D x 50 mm L) and a rectangular quartz cell (path length 50 mm). Single crystal X-ray diffraction experiments were performed on a Rigaku RAXIS-RAPID diffractometer using graphite monochromated Mo-Kα radiation. The structure was solved by direct methods [20] and expanded using Fourier techniques. The non-hydrogen atoms were refined anisotropically. Hydrogen atoms were refined using the riding model. All calculations were performed using the CrystalStructure [21] crystallographic software package.

### *2.1. Preparation of optically active glycerol analogues [(S)-**1**, and (S)-**6**, (R)-**7**, and (R)-**8a**]*

#### *2.1.1. (S)-3-(Benzyloxy)propane-1,2-diol [(S)-**1**] [8–11]*

To a solution of (*R*)-(2,2-dimethyl-1,3-dioxolan-4-yl)methanol [(*R*)-**3**] (3.00 mL, 24.3 mmol) in anhydrous DMF (40 mL) were added NaH (50–72 % in mineral oil, 1.28 g, 26.7 mmol) and benzyl bromide (3.20 mL, 26.7 mmol) at 0 °C under argon. The reaction mixture was stirred at room temperature for 1.5 h under argon. Then 10 % $NH_4Cl$ aq. (40 mL) was added and then extracted with *n*-hexane–AcOEt (1:5, 100 mL × 3). The extract was washed with water (100 mL), dried over anhydrous $MgSO_4$, filtered, and concentrated *in vacuo* to afford (*R*)-4-[(benzyloxy) methyl]-2,2-dimethyl-1,3-dioxolane [(*R*)-**4**], which was used in the next reaction without further purification. To a solution of (*R*)-**4** in THF (20 mL) was added 1 N HCl (20 mL), and the mixture was stirred at room temperature for 3.5 h, and then extracted with AcOEt (40 mL × 4). The extract was dried over anhydrous $MgSO_4$, filtered, and concentrated *in vacuo*. The oily residue was purified by silica gel column chromatography [Silica Gel PSQ 60B: *n*-hexane–AcOEt (1:2)] to afford (*S*)-**1** (4.10 g, 93 %). Colorless oil; $[\alpha]_D^{27}$ + 3.0 (*c* 1.00, $CHCl_3$); $^1$H NMR (500 MHz, $CDCl_3$) δ 2.06 (brs, 1H), 2.57 (d, *J* = 4.5 Hz, 1H), 3.55 (dd, *J* = 6.2, 9.7 Hz, 1H), 3.58 (dd, *J* = 4.1, 9.7 Hz, 1H), 3.60–3.66 (m, 1H), 3.67–3.74 (m, 1H), 3.86–3.92 (m, 1H), 4.55 (s, 2H), 7.27–7.37 (m, 5H); $^{13}$C NMR (125 MHz, $CDCl_3$) δ 64.0, 70.8, 71.6, 73.5, 127.79, 127.84, 128.5, 137.7; IR (neat) 3392, 2870, 1717, 1653, 1454 $cm^{-1}$; HRMS (ESI): *m/z* [M + Na]$^+$ calcd for $C_{10}H_{14}O_3Na$: 205.0841; found, 205.0842.

#### *2.1.2. (S)-3-Methoxypropan-1,2-diol [(S)-**6**] [22]*

To a solution of (*R*)-(2,2-dimethyl-1,3-dioxolan-4-yl)methanol [(*R*)-**3**] (3.00 mL, 24.3 mmol) in anhydrous DMF (40 mL) was added NaH (50–72 % in mineral oil, 1.28 g, 26.7 mmol) and methyl iodide (1.70 mL, 26.7 mmol) at 0 °C under argon. The reaction mixture was stirred at room temperature for 2 h under argon. Then 10 % $NH_4Cl$ aq. (40 mL) was added and then extracted with *n*-hexane–AcOEt (1:5, 100 mL × 2). The extract was washed with sat. $Na_2S_2O_3$ aq. (60 mL), dried over anhydrous $MgSO_4$, filtered, and concentrated *in vacuo* to afford (*R*)-4-(methoxymethyl)-2,2-dimethyl-1,3-dioxolane [(*R*)-**5**], which was used in the next reaction without further purification. To a solution of (*R*)-**5** in THF (20 mL) was added 1 N HCl (20 mL), and the mixture was stirred at room temperature for 2 h. The reaction mixture was concentrated *in vacuo*, and the oily residue was purified by silica gel column chromatography [Silica Gel PSQ 60B: $CHCl_3$–MeOH (20:1)] to afford (*S*)-**6** (2.40 g, 93 %). (*S*)-**6**: pale yellow oil; $[\alpha]_D^{19}$ + 4.5 (*c* 1.00, $CHCl_3$); $^1$H NMR (500 MHz, $CDCl_3$) δ 2.11 (dd, *J* = 5.3, 6.9 Hz, 1H), 2.59 (d, *J* = 4.9 Hz, 1H), 3.40 (s, 3H), 3.45–3.52 (m, 2H), 3.61–3.67 (m, 1H), 3.69–3.74 (m, 1H), 3.84–3.90 (m, 1H); $^{13}$C NMR (125 MHz, $CDCl_3$) δ 59.2, 64.0, 70.7, 74.2; IR (neat) 3382, 2891, 1456, 1129 $cm^{-1}$; MS (ESI): *m/z* [M + Na]$^+$ 129.10.

#### *2.1.3. (R)-{[(3-Methoxypropane-1,2-diyl)bis(oxy)]bis(methylene)} dibenzene [(R)-**7**]*

To a solution of (*S*)-3-methoxypropane-1,2-diol [(*S*)-**6**] (506 mg, 4.77 mmol) in anhydrous DMF (17 mL) were added NaH (50–72 % in mineral oil, 456 mg, 9.54 mmol) and benzyl bromide (1.10 mL, 9.54 mmol) at 0 °C under argon. The reaction mixture was stirred at room temperature for 1 h under argon. Then 10 % $NH_4Cl$ aq. (15 mL) was added and then extracted with *n*-hexane–AcOEt (1:5, 50 mL × 3). The extract was washed with water (60 mL), dried over anhydrous $MgSO_4$, filtered, and concentrated *in vacuo*. The oily residue was purified by silica gel column chromatography [Silica Gel PSQ 60B: *n*-hexane–AcOEt (3:1)] to afford (*R*)-**7** (1.18 g, 86 %). (*R*)-**7**: colorless oil; $[\alpha]_D^{17}$ + 6.2 (*c* 1.00, $CHCl_3$); $^1$H NMR (500 MHz, $CDCl_3$) δ 3.36 (s, 3H), 3.50–3.64 (m, 4H), 3.74–3.79 (m, 1H), 4.54 (s, 2H), 4.70 (s, 2H), 7.25–7.37 (m, 10*H*); $^{13}$C NMR (125 MHz, $CDCl_3$) δ 59.3, 70.3, 72.2, 72.9, 73.4, 127.5, 127.55, 127.58, 127.7, 128.28, 128.33, 138.3, 138.6; IR (neat) 3298, 3030, 2875, 1454, 1104 $cm^{-1}$; HRMS (ESI): *m/z* [M + Na]$^+$ calcd for $C_{18}H_{22}O_3Na$: 309.1467; found, 309.1470.

#### *2.1.4. (R)-1-(Benzyloxy)-3-methoxypropan-2-ol [(R)-**8a**] [23]*

To a solution of (*S*)-3-methoxypropan-1,2-diol [(*S*)-**6**] (940 mg, 8.56 mmol) in anhydrous $CH_2Cl_2$ (30 mL) were added $Ag_2O$ (2.98 g, 12.9 mmol) and benzyl bromide (1.35 mL, 12.9 mmol) at room temperature under argon. The reaction mixture was stirred at room temperature for 16 h under argon, and then filtered and concentrated *in vacuo*. The oily residue was purified by silica gel column chromatography [Silica Gel PSQ 60B: *n*-hexane–AcOEt (3:1)] to afford an inseparable mixture of (*R*)-1-(benzyloxy)-3-methoxypropan-2-ol [(*R*)-**8a**] and (*S*)-2-(benzyloxy)-3-methoxypropan-1-ol [(*S*)-**8b**] (880 mg, 51 %). To the mixture of (*R*)-**8a** and (*S*)-**8b** (720 mg, 3.67 mmol) in DMF (13 mL) were added imidazole (300 mg, 4.40 mmol) and *tert*-butyldiphenylsilyl chloride (473 μL, 1.84 mmol) at room temperature under argon. The reaction mixture was stirred at room temperature for 6 h under argon, and then 1 N HCl (13 mL) was added. The mixture was extracted with *n*-hexane–AcOEt (1:5, 45 mL × 3), and then the extract was washed with water (45 mL), dried over anhydrous $MgSO_4$, filtered, and concentrated *in vacuo*. The oily

**Table 1**
Crystal data of (*S*)-**10**, (*S*)-**13**, and (*S*)-**14**.

| | (*S*)-**10** | (*S*)-**13** | (*S*)-**14** |
|---|---|---|---|
| Chemical formula | $C_5H_8O_5$ | $C_9H_{12}O_3$ | $C_{10}H_{17}NO_4$ |
| Formula weight | 148.12 | 168.19 | 215.25 |
| Crystal system, space group | Monoclinic<br>*C*2 (No. 5) | Orthorhombic<br>$P2_12_12_1$ (No. 19) | Orthorhombic<br>$P2_12_12_1$ (No. 19) |
| *a*, *b*, *c* (Å) | *a* = 22.791(2)<br>*b* = 4.1949(3)<br>*c* = 7.0207(7) | *a* = 5.06740(17)<br>*b* = 7.7275(2)<br>*c* = 20.9629(7) | *a* = 7.9836(3)<br>*b* = 11.8520(5)<br>*c* = 12.2143(6) |
| β (°) | 100.628(3) | | |
| *V* (Å$^3$) | 659.70(11) | 820.87(5) | 1155.73(9) |
| *Z* | 4 | 4 | 4 |
| Calculated density (g/cm$^3$) | 1.491 | 1.361 | 1.237 |
| μ(Mo-Kα) (cm$^{-1}$) | 1.361 | 1.014 | 0.951 |
| Crystal size (mm) | 0.500 × 0.400 × 0.100 | 0.400 × 0.300 × 0.250 | 0.300 × 0.250 × 0.100 |

residue was purified by silica gel column chromatography [Silica Gel PSQ 60B: *n*-hexane–AcOEt (2:1)] to afford (*R*)-[2-(benzyloxy)-3-methoxypropoxy](*tert*-butyl)diphenylsilane [(*R*)-**9**] (910 mg, ca. 36 %) and unreacted (*R*)-**8a** (335 mg, 47 %). (*R*)-**8a**: colorless oil; $[\alpha]_D^{24}$ + 3.6 (*c* 1.00, $CHCl_3$); $^1$H NMR (500 MHz, $CDCl_3$) *δ* 2.46 (brs, 1H), 3.38 (s, 3H), 3.43 (dd, *J* = 6.3, 9.7 Hz, 1H), 3.48 (dd, *J* = 4.3, 9.7 Hz, 1H), 3.50 (dd, *J* = 6.3, 9.7 Hz, 1H), 3.55 (dd, *J* = 4.4, 9.7 Hz, 1H), 3.96–4.02 (m, 1H), 4.56 (s, 2H), 7.27–7.37 (m, 5H); $^{13}$C NMR (125 MHz, $CDCl_3$) *δ* 59.2, 69.5, 71.4, 73.5, 73.8, 127.7, 127.8, 128.4, 138.0; IR (neat) 3464, 2878, 1451, 1196, 1111 cm$^{-1}$; HRMS (ESI): *m/z* $[M + Na]^+$ calcd for $C_{11}H_{16}O_3Na$: 219.0997; found, 219.1016.

### 2.2. Preparation of optically active L-malic acid analogues [(S)-10, (S)-11, and (S)-12]

#### 2.2.1. (S)-3-Hydroxy-4-methoxy-4-oxobutanoic acid [(S)-10] [24]

A solution of L-malic acid [(*R*)-**2**] (3.54 g, 26.3 mmol) in trifluoroacetic anhydride (15 mL) was stirred at room temperature for 40 min under argon, and then concentrated *in vacuo*. MeOH (15 mL) was added to the residue, and the stirring was continued at room temperature for 1.5 h. The reaction mixture was concentrated *in vacuo*, and the crude product was washed with *n*-hexane to afford (*S*)-**10** (2.87 g, 73 %). (*S*)-**10**: colorless needles ($Et_2O$–*n*-hexane); mp 73.2–74.0 °C; $[\alpha]_D^{22}$ − 5.6 (*c* 1.00, MeOH); $^1$H NMR (500 MHz, $CDCl_3$) *δ* 2.86 (dd, *J* = 6.2, 16.8 Hz, 1H), 2.94 (dd, *J* = 4.2, 16.8 Hz, 1H), 3.83 (s, 3H), 4.51–4.54 (m, 1H); $^{13}$C NMR (125 MHz, $CDCl_3$) *δ* 38.3, 53.0, 66.9, 173.6, 175.6; IR (KBr) 3439, 2959, 1740, 1440, 1401, 1223, 1181, 1119 cm$^{-1}$; HRMS (ESI): *m/z* $[M-H]^-$ calcd for $C_5H_7O_5$: 147.0293; found, 147.0289. Anal. Calcd for $C_5H_8O_5$: C, 40.55; H, 5.44. Found: C, 40.25; H, 5.34 %.

#### 2.2.2. Dimethyl (S)-2-hydroxysuccinate [(S)-11] [25]

Thionyl chloride (1.10 mL, 14.9 mmol) and MeOH (5 mL) were mixed and stirred at –10 °C for 10 min. L-Malic acid [(*R*)-**2**] (1.00 g, 7.46 mmol) was added and the mixture was stirred at room temperature for 2 h. The reaction mixture was concentrated *in vacuo*, and the oily residue was purified by silica gel column chromatography [Silica Gel PSQ 60B: $CHCl_3$–MeOH (9:1)] to afford (*S*)-**11** (1.17 g, 95 %). (*S*)-**11**: colorless oil; $[\alpha]_D^{22}$ + 3.7 (*c* 1.00, $CHCl_3$); $^1$H NMR (500 MHz, $CDCl_3$) *δ* 2.81 (dd, *J* = 6.2, 16.4 Hz, 1H), 2.87 (dd, *J* = 4.3, 16.4 Hz, 1H), 3.21 (d, *J* = 5.3 Hz, 1H), 3.72 (s, 3H), 3.82 (s, 3H), 4.51 (q, *J* = 5.3 Hz, 1H); $^{13}$C NMR (125 MHz, $CDCl_3$) *δ* 38.5, 52.1, 52.9, 62.3, 171.1, 173.8; IR (neat) 3488, 2957, 1740, 1439, 1275, 1109 cm$^{-1}$; HRMS (ESI): *m/z* $[M + Na]^+$ calcd for $C_6H_{10}O_5Na$: 185.0426; found, 185.0420.

#### 2.2.3. Dimethyl (S)-2-methoxysuccinate [(S)-12] [26]

To a solution of (*S*)-**11** (934 mg, 5.76 mmol) in anhydrous $CH_2Cl_2$ (30 mL) were added $Ag_2O$ (1.60 g, 6.90 mmol) and methyl iodide (4 mL, 64.2 mmol) at room temperature under argon. The reaction mixture was stirred at room temperature for 24 h under argon, and then filtered and concentrated *in vacuo*. The oily residue was purified by silica gel column chromatography [Silica Gel PSQ 60B: *n*-hexane–AcOEt (3:1)] to afford (*S*)-**12** (661 mg, 65 %). (*S*)-**12**: colorless oil; $[\alpha]_D^{17}$ –44.8 (*c* 1.00, $CHCl_3$); $^1$H NMR (500 MHz, $CDCl_3$) *δ* 2.74 (dd, *J* = 7.8, 16.1 Hz, 1H), 2.79 (dd, *J* = 4.9, 16.1 Hz, 1H), 3.47 (s, 3H), 3.72 (s, 3H), 3.79 (s, 3H), 4.21 (dd, *J* = 4.9, 7.8 Hz, 1H); $^{13}$C NMR (125 MHz, $CDCl_3$) *δ* 37.6, 52.0, 52.3, 58.9, 76.7, 170.5, 171.8; IR (neat) 2956, 2836, 1740, 1282, 1129 cm$^{-1}$; HRMS (ESI): *m/z* $[M + Na]^+$ calcd for $C_7H_{12}O_5Na$: 199.0582; found, 199.0570.

### 2.3. Single crystal X-ray structure analysis of (S)-3-hydroxy-4-methoxy-4-oxobutanoic acid [(S)-10], (S)-3-phenoxypropane-1,2-diol [(S)-13], and (S)-1-[(2-methylpropan-2-yl)oxycarbonyl]pyrrolidine-2-carboxylic acid [Boc-L-Pro-OH, (S)-14]

The data of (*S*)-**10** (colorless needle) were collected at a temperature of − 150 ± 1 °C to a maximum 2θ value of 54.8°. A total of 44 oscillation images were collected. A sweep of data was done using ω scans from 130.0° to 190.0° in 5.00° steps, at χ = 45.0° and ϕ = 0.0°. The exposure rate was 131.0 [sec./°]. A second sweep was performed using ω scans from 0.0° to 160.0° in 5.00° steps, at χ = 45.0° and ϕ = 180.0°. The exposure rate was 131.0 [sec./°]. The crystal-to-detector distance was 127.40 mm. Readout was performed in the 0.100 mm pixel mode. The data of (*S*)-**13** (colorless needle) were collected at a temperature of − 150 ± 1 °C to a maximum 2θ value of 54.9°. A total of 44 oscillation images were collected. A sweep of data was done using ω scans from 130.0° to 190.0° in 5.00° steps, at χ = 45.0° and ϕ = 30.0°. The exposure rate was 135.0 [sec./°]. A second sweep was performed using ω scans

**Table 2**
Data collection of (*S*)-**10**, (*S*)-**13**, and (*S*)-**14**.

| | (*S*)-**10** | (*S*)-**13** | (*S*)-**14** |
|---|---|---|---|
| Diffractometer | Rigaku RAXIS-RAPID | Rigaku RAXIS-RAPID | Rigaku RAXIS-RAPID |
| Absorption correction | Multi-scan | Multi-scan | Multi-scan |
| $T_{min}$, $T_{max}$ | 0.646, 0.986 | 0.879, 0.975 | 0.845, 0.991 |
| No. of measured and independent reflections | 3216, 1493 | 7945, 1861 | 11322, 2628 |
| $R_{int}$ | 0.0212 | 0.0132 | 0.0408 |

**Table 3**
Data refinement of (*S*)-**10**, (*S*)-**13**, and (*S*)-**14**.

| | (*S*)-**10** | (*S*)-**13** | (*S*)-**14** |
|---|---|---|---|
| Final *R* indices [I > 2.00σ(I)], *S* | $R_1 = 0.0273$, $wR_2 = 0.1036$ $S = 0.834$ | $R_1 = 0.0278$, $wR_2 = 0.1005$ $S = 0.954$ | $R_1 = 0.0391$, $wR_2 = 0.1441$ $S = 1.023$ |
| No. of reflections | 1493 | 1861 | 2628 |
| No. of parameters | 93 | 111 | 137 |
| H-atom treatment | Constrained refinement | Constrained refinement | Constrained refinement |
| $\Delta\rho_{max}$, $\Delta\rho_{min}$ (e Å$^{-3}$) | 0.21, –0.14 | 0.27, –0.17 | 0.25, –0.25 |

**Table 4**
Hydrogen bond geometry of (*S*)-**10**, (*S*)-**13**, and (*S*)-**14**.

| D–H···A | D–H (Å) | H···A (Å) | D···A (Å) | D–H···A (°) | Symmetry codes |
|---|---|---|---|---|---|
| (*S*)-**10** | | | | | |
| O(1)–H(1)···O(2) | 0.84 | 1.833 | 2.663(2) | 169.29 | –X + 1/2 + 1, Y + 1/2–1, –Z |
| O(3)–H(2)···O(1) | 0.84 | 1.954 | 2.782(2) | 168.35 | –X + 2, Y, –Z + 1 |
| (*S*)-**13** | | | | | |
| O(1)–H(1)···O(2) | 0.84 | 1.971 | 2.7896(13) | 164.43 | –X + 2, Y + 1/2–1, –Z + 1/2 |
| O(2)–H(2)···O(1) | 0.84 | 1.912 | 2.7474(13) | 172.59 | X + 1, Y, Z |
| (*S*)-**14** | | | | | |
| O(2)–H(2)···O(3) | 0.84 | 1.792 | 2.631(3) | 177.33 | –X, Y + 1/2, –Z + 1/2 |

from 0.0° to 160.0° in 5.00° steps, at χ = 45.0° and ϕ = 180.0°. The exposure rate was 135.0 [sec./°]. The crystal-to-detector distance was 127.40 mm. Readout was performed in the 0.100 mm pixel mode. The data of (*S*)-**14** (colorless plate) were collected at a temperature of − 150 ± 1 °C to a maximum 2θ value of 54.8°. A total of 44 oscillation images were collected. A sweep of data was done using ω scans from 130.0° to 190.0° in 5.00° steps, at χ = 45.0° and ϕ = 0.0°. The exposure rate was 136.0 [sec./°]. A second sweep was performed using ω scans from 0.0° to 160.0° in 5.00° steps, at χ = 45.0° and ϕ = 180.0°. The exposure rate was 136.0 [sec./°]. The crystal-to-detector distance was 127.40 mm. Readout was performed in the 0.100 mm pixel mode. The crystallographic data for (*S*)-**10**, (*S*)-**13**, and (*S*)-**14** are summarized in Tables 1–4.

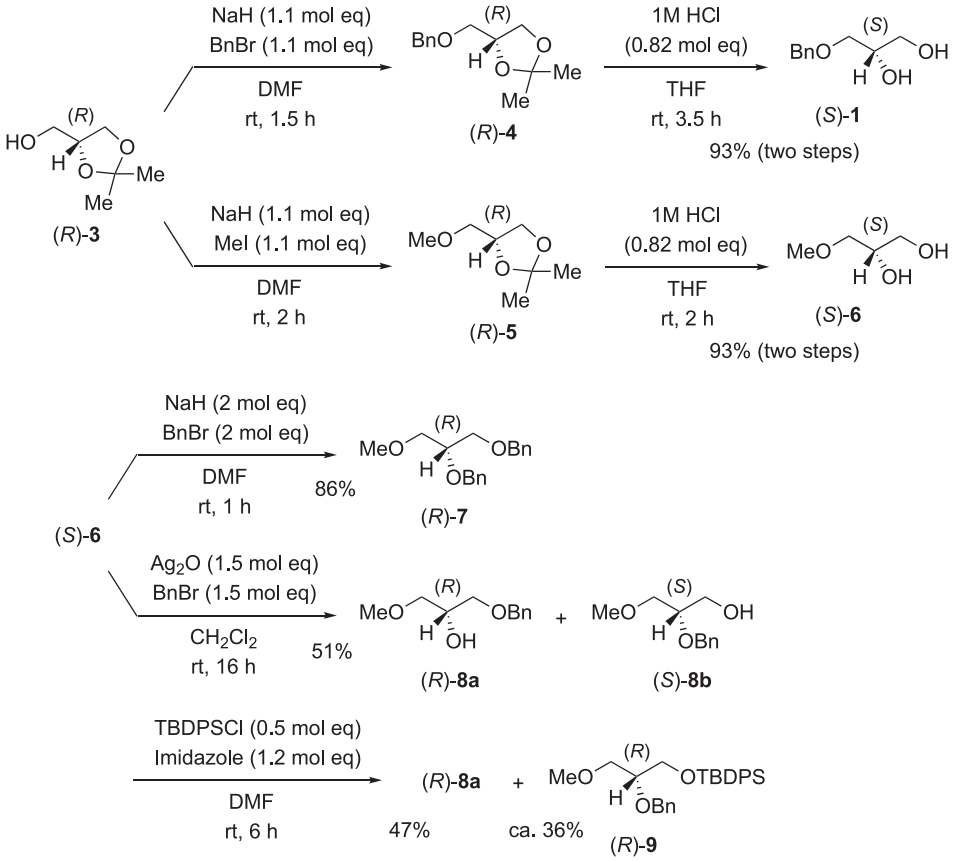


**Scheme 1.** Synthesis of (*S*)-**1**, (*S*)-**6**, (*R*)-**7**, and (*R*)-**8a**.

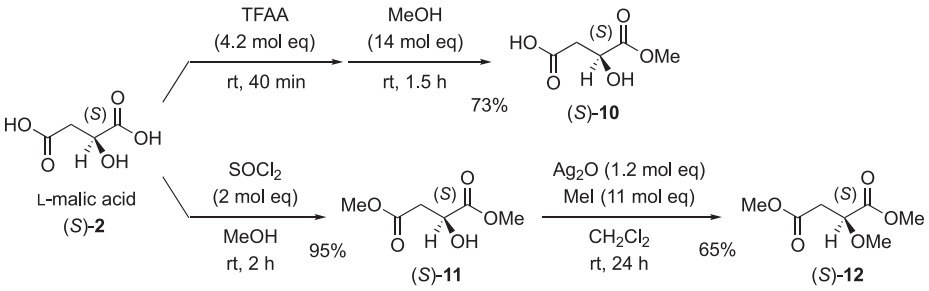


**Scheme 2.** Synthesis of (*S*)-**10**, (*S*)-**11**, and (*S*)-**12**.

**Table 5**
Specific rotation of (*S*)-3-(benzyloxy)propane-1,2-diol [(*S*)-**1**] and its analogues [(*S*)-**6**, (*S*)-**13**, (*R*)-**8a**, and (*R*)-**7**]

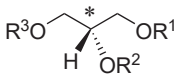

(*S*)-**1** : $R^1 = R^2 = H$, $R^3 = Bn$
(*S*)-**6** : $R^1 = R^2 = H$, $R^3 = Me$
(*S*)-**13** : $R^1 = R^2 = H$, $R^3 = Ph$
(*R*)-**8a** : $R^1 = Bn$, $R^2 = H$, $R^3 = Me$
(*R*)-**7** : $R^1 = R^2 = Bn$, $R^3 = Me$

.

| Conc (g/100 mL) | $[\alpha]_D^T$ of (*S*)-**1** ($CHCl_3$) | $[\alpha]_D^T$ of (*S*)-**6** ($CHCl_3$) | $[\alpha]_D^T$ of (*S*)-**13** ($CHCl_3$) | $[\alpha]_D^T$ of (*R*)- **8a** ($CHCl_3$) | $[\alpha]_D^T$ of (*R*)-**7** ($CHCl_3$) |
|---|---|---|---|---|---|
| 0.10 | +3.9 (27 °C) | +5.5 (19 °C) | +4.8 (25 °C) | +1.7 (23 °C) | +5.2 (19 °C) |
| 0.30 | +2.8 (26 °C) | +5.2 (20 °C) | +3.1 (25 °C) | +2.6 (23 °C) | +5.7 (19 °C) |
| 0.50 | +3.8 (27 °C) | +6.1 (19 °C) | +3.4 (27 °C) | +3.3 (24 °C) | +6.5 (17 °C) |
| 1.0 | +3.0 (27 °C) | +4.5 (19 °C) | +3.0 (27 °C) | +3.6 (24 °C) | +6.2 (17 °C) |
| 10 | –3.3 (27 °C) | –4.1 (19 °C) | –5.6 (26 °C) | +3.8 (24 °C) | +5.7 (17 °C) |
| 20 | –5.6 (28 °C) | –5.3 (19 °C) | –7.3 (26 °C) | +3.9 (24 °C) | +5.4 (17 °C) |
| Conc (g/100 mL) | $[\alpha]_D^T$ of (*S*)-**1**(MeOH) | $[\alpha]_D^T$ of (*S*)-**6**(MeOH) | $[\alpha]_D^T$ of (*S*)-**13**(acetone) | $[\alpha]_D^T$ of (*R*)- **8a**(MeOH) | $[\alpha]_D^T$ of (*R*)-**7**(MeOH) |
| 0.10 | +2.1 (26 °C) | +4.6 (19 °C) | +2.1 (24 °C) | +4.6 (22 °C) | +1.8 (18 °C) |
| 0.30 | +1.7 (26 °C) | +5.7 (19 °C) | +1.9 (24 °C) | +4.4 (22 °C) | +1.6 (19 °C) |
| 0.50 | +2.4 (27 °C) | +6.5 (17 °C) | +1.9 (25 °C) | +4.3 (21 °C) | +4.8 (18 °C) |
| 1.0 | +2.1 (26 °C) | +6.2 (18 °C) | +2.1 (25 °C) | +4.7 (19 °C) | +3.2 (18 °C) |
| 10 | +1.3 (26 °C) | +5.7 (18 °C) | +1.4 (25 °C) | +3.9 (20 °C) | +1.7 (18 °C) |
| 20 | +0.9 (26 °C) | +5.2 (18 °C) | +0.7 (25 °C) | +4.2 (21 °C) | +1.2 (18 °C) |

**Table 6**
Specific rotation of L-malic acid [(*S*)-**2**] analogues [(*S*)-**10**, (*S*)-**11**, and (*S*)-**12**]

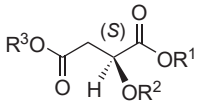

(*S*)-**10** : $R^1 = Me$, $R^2 = R^3 = H$
(*S*)-**11** : $R^1 = R^3 = Me$, $R^3 = H$
(*S*)-**12** : $R^1 = R^2 = R^3 = Me$

.

| Conc (g/100 mL) | $[\alpha]_D^T$ of (*S*)-**10**($CHCl_3$) | $[\alpha]_D^T$ of (*S*)-**11** ($CHCl_3$) | $[\alpha]_D^T$ of (*S*)-**12** ($CHCl_3$) |
|---|---|---|---|
| 0.10 | | +3.9 (21 °C) | –44.4 (17 °C) |
| 0.30 | | +3.9 (21 °C) | –43.6 (17 °C) |
| 0.50 | | +3.1 (22 °C) | –44.5 (17 °C) |
| 1.0 | | +3.7 (22 °C) | –44.8 (17 °C) |
| 10 | | +2.6 (23 °C) | |
| 20 | | +1.9 (23 °C) | |
| 40 | | +0.3 (23 °C) | |
| 60 | | –1.2 (24 °C) | |
| Conc (g/100 mL) | $[\alpha]_D^T$ of (*S*)-**10**(MeOH) | $[\alpha]_D^T$ of (*S*)-**11**(MeOH) | $[\alpha]_D^T$ of (*S*)-**12**(MeOH) |
| 0.10 | –4.6 (21 °C) | –9.6 (17 °C) | |
| 0.30 | –5.5 (21 °C) | –8.8 (17 °C) | |
| 0.50 | –5.6 (21 °C) | –9.2 (17 °C) | |
| 1.0 | –5.6 (22 °C) | –8.1 (17 °C) | |
| 10 | –5.5 (22 °C) | –8.5 (16 °C) | |
| 20 | –5.2 (22 °C) | –8.6 (16 °C) | |
| 40 | –4.7 (22 °C) | –8.5 (15 °C) | |
| 60 | –3.9 (22 °C) | | |

**Table 7**
Specific rotation of (*S*)-**14**, (*R*)-**15**, (*R*)-**16**, (*S*)-**17**, (*R*)-**18**, and (*S*)-**19**

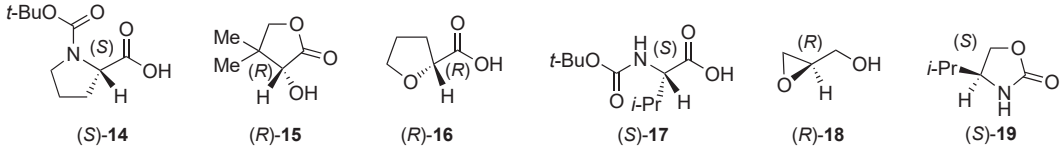


(*S*)-**14** (*R*)-**15** (*R*)-**16** (*S*)-**17** (*R*)-**18** (*S*)-**19**

.

| Conc (g/100 mL) | $[\alpha]_D^T$ of (*S*)-**14** ($CHCl_3$) | $[\alpha]_D^T$ of (*R*)-**15** ($CHCl_3$) | $[\alpha]_D^T$ of (*R*)-**16** ($CHCl_3$) | $[\alpha]_D^T$ of (*S*)-**17** ($CHCl_3$) | $[\alpha]_D^T$ of (*R*)-**18** ($CHCl_3$) | $[\alpha]_D^T$ of (*S*)-**19** ($CHCl_3$) |
|---|---|---|---|---|---|---|
| 0.01 | –166.6 (25 °C) | | +51.2 (27 °C) | | | |
| 0.05 | –154.4 (24 °C) | | +46.2 (26 °C) | | | |
| 0.10 | –141.8 (24 °C) | –15.6 (26 °C) | +45.3 (27 °C) | +15.2 (27 °C) | +24.3 (24 °C) | –2.3 (26 °C) |
| 0.30 | –125.8 (24 °C) | –15.9 (27 °C) | +39.8 (26 °C) | +10.7 (27 °C) | +23.0 (24 °C) | +0.9 (25 °C) |
| 0.50 | –125.4 (24 °C) | –16.8 (26 °C) | +35.8 (26 °C) | +8.1 (26 °C) | +23.8 (25 °C) | +3.6 (26 °C) |
| 1.0 | –111.2 (24 °C) | –17.9 (27 °C) | +29.4 (26 °C) | +8.0 (26 °C) | +23.1 (25 °C) | +6.8 (26 °C) |
| 5.0 | | –25.0 (27 °C) | +18.2 (26 °C) | | | +15.2 (26 °C) |
| 10 | –73.3 (26 °C) | –30.5 (26 °C) | +12.5 (26 °C) | +7.4 (26 °C) | +19.6 (26 °C) | +16.8 (26 °C) |
| 20 | –65.5 (26 °C) | –34.1 (27 °C) | +14.0 (26 °C) | +6.1 (26 °C) | +17.6 (26 °C) | +16.2 (26 °C) |
| 50 | | | | +5.3 (26 °C) | +15.0 (25 °C) | |
| Conc (g/100 mL) | $[\alpha]_D^T$ of (*S*)-**14**(MeOH) | $[\alpha]_D^T$ of (*R*)-**15**(MeOH) | $[\alpha]_D^T$ of (*R*)-**16**(MeOH) | $[\alpha]_D^T$ of (*S*)-**17**(MeOH) | $[\alpha]_D^T$ of (*R*)-**18**(MeOH) | $[\alpha]_D^T$ of (*S*)-**19**(MeOH) |
| 0.01 | –45.4 (27 °C) | | | | | |
| 0.05 | –52.5 (27 °C) | | | | | |
| 0.10 | –52.3 (28 °C) | –26.9 (26 °C) | +2.8 (26 °C) | –3.0 (27 °C) | +11.9 (25 °C) | –23.5 (26 °C) |
| 0.30 | –52.7 (28 °C) | –28.4 (26 °C) | +1.9 (26 °C) | –3.4 (27 °C) | +12.7 (25 °C) | –23.9 (25 °C) |
| 0.50 | –57.0 (27 °C) | –28.6 (26 °C) | +1.1 (26 °C) | –3.4 (27 °C) | +12.5 (25 °C) | –24.7 (26 °C) |
| 1.0 | –54.9 (27 °C) | –27.5 (26 °C) | +2.0 (26 °C) | –2.7 (27 °C) | +11.8 (25 °C) | –21.9 (26 °C) |
| 5.0 | | –28.2 (26 °C) | | | | –22.6 (26 °C) |
| 10 | –53.0 (27 °C) | –28.6 (26 °C) | +3.4 (26 °C) | –1.6 (27 °C) | +12.0 (25 °C) | –21.6 (26 °C) |
| 20 | –51.9 (27 °C) | –29.0 (26 °C) | +4.1 (26 °C) | –0.2 (27 °C) | +12.3 (25 °C) | –18.2 (27 °C) |
| 40 | –45.8 (27 °C) | –30.8 (26 °C) | +4.3 (26 °C) | +2.0 (26 °C) | +12.8 (25 °C) | –16.9 (25 °C) |
| 50 | | | +4.9 (26 °C) | +3.0 (26 °C) | +12.8 (26 °C) | |
| 60 | | –32.7 (26 °C) | +5.8 (26 °C) | +4.5 (27 °C) | +13.4 (26 °C) | –13.5 (25 °C) |

## 3. Results and discussion

### *3.1. Synthesis of optically active glycerol analogues and structurally related compounds*

#### *3.1.1. Synthesis of (S)-3-(benzyloxy)propane-1,2-diol [(S)-1] and its analogues*

Optically active glycerol analogue (*S*)-**1** and its structurally related compounds (*S*)-**6**, (*R*)-**7**, and (*R*)-**8a** were synthesized from (*R*)-2,2-dimethyl-1,3-dioxolan-4-methanol [(*R*)-**3**] as shown in Scheme 1. Commercially available (*R*)-**3** was benzylated with benzyl bromide in the presence of sodium hydride to give (*R*)-**4**, which was deprotected using 1 M HCl aq. to afford (*S*)-**1**. Structurally related (*S*)-**6** was also obtained by methylation of (*R*)-**3** with methyl iodide, and subsequent deprotection of the resultant (*R*)-**5** under acidic conditions. Diol (*S*)-**6** was successfully transformed to dibenzylated (*R*)-**7** with benzyl bromide. On the other hand, monobenzylation of (*S*)-**6** with benzyl bromide in the presence of $Ag_2O$ gave an inseparable mixture of 1-benzyloxy-derivative (*R*)-**8a** and 2-benzyloxy-derivative (*S*)-**8b**. To isolate (*R*)-**8a**, the mixture was silylated with *tert*-butyldiphenylsilyl chloride (TBDPSCl) to afford silyl ether (*R*)-**9** and unreacted (*R*)-**8a**.

#### *3.1.2. Synthesis of optically active L-malic acid [(S)-2] analogues*

Optically active (*S*)-**10**, (*S*)-**11**, and (*S*)-**12** were synthesized from L-malic acid [(*S*)-**2**] as shown in Scheme 2. (*S*)-**2** was treated with trifluoroacetic anhydride (TFAA), followed by methanolysis to afford monoester (*S*)-**10**. Diester (*S*)-**11** was obtained by the esterification of (*S*)-**2** using thionyl chloride in MeOH. Methylation of (*S*)-**11** was achieved using methyl iodide and $Ag_2O$ to give (*S*)-**12**.

### *3.2. Specific rotation of optically active glycerol analogues and structurally related compounds*

Specific rotations of optically active glycerol analogue (*S*)-**1** and its structurally related compounds (*S*)-**6**, (*S*)-**13**, (*R*)-**8a**, and (*R*)-**7** were measured in $CHCl_3$ and MeOH at different concentrations (Table 5). Since (*S*)-**13** is not sufficiently soluble in MeOH, acetone was used to measure specific rotations. In general, slightly polar solvents such as $CHCl_3$ have little effect on molecular geometry, but protic solvents such as MeOH are known to readily break intermolecular hydrogen bonds [27]. The specific rotation of (*S*)-**1** in $CHCl_3$ markedly changed from

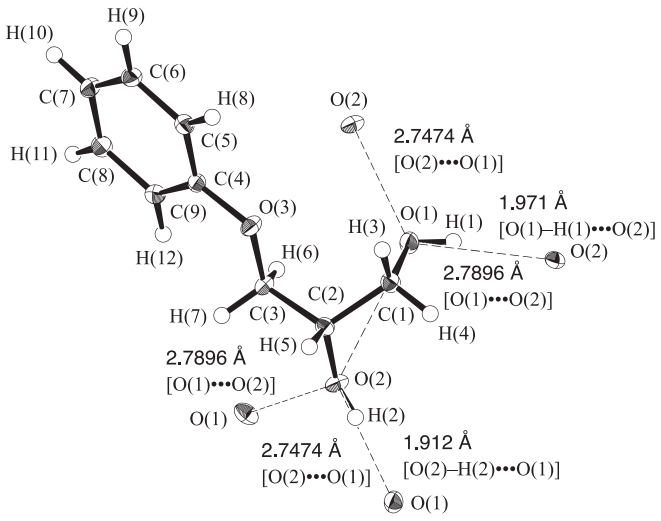


**Fig. 2.** ORTEP drawing of (*S*)-**13**.

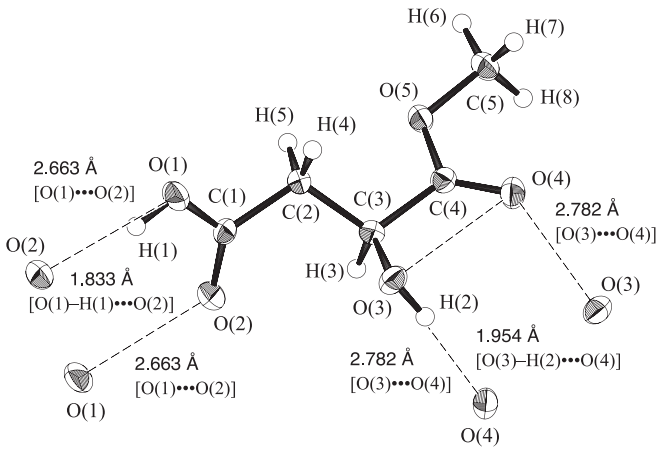


**Fig. 3.** ORTEP drawing of (*S*)-**10**.

+3.9 (*c* 0.10) to –5.6 (*c* 20.0) depending on the concentration. Significant concentration-dependent changes in specific rotations were also observed for (*S*)-**6** and (*S*)-**13** in $CHCl_3$. All these compounds have hydroxy groups at the C1 and C2 positions in the C3 carbon chain. On the other hand, the specific rotations of (*R*)-**8a**, which has a hydroxy group at the C2 position, showed slight changes depending on the concentration. While the specific rotations of (*R*)-**7**, which has no hydroxy group, showed almost no concentration-dependent changes in $CHCl_3$. Concentration-dependent changes in the specific rotations of a series of compounds were greatly attenuated when methanol and acetone were used as solvents. The hydroxy group of methanol could be a hydrogen-bond donor and/or acceptor, and acetone has carbonyl groups that could be hydrogen-bond acceptors. Therefore, the formation of aggregates via intermolecular hydrogen bonding under high concentration conditions is one of the factors responsible for the concentration-dependent change in specific rotation.

Specific rotations of (*S*)-**10**, (*S*)-**11**, and (*S*)-**12**, which are structurally related to L-malic acid [(*S*)-**2**], were measured in $CHCl_3$ and/or MeOH at different concentrations (Table 6). (*S*)-**10** was insoluble in $CHCl_3$, but its specific rotation showed a slight, concentration-dependent change in MeOH. The specific rotation of (*S*)-**11** changed little at each concentration in MeOH, but a pronounced concentration-dependent change from + 3.9 (*c* 0.30) to –1.2 (*c* 60.0) was observed in $CHCl_3$. On the other hand, the specific rotation of (*S*)-**12** in $CHCl_3$ did not change at all at any concentration. These results correlate with the presence or absence of hydroxy or carboxy groups that could be hydrogen-bond donors or acceptors.

Based on chemical structural similarity to these glycerol and L-malic acid analogues, specific rotations of several kinds of optically active organic compounds were also measured in $CHCl_3$ and/or MeOH at different concentrations (Table 7). As a result, we found that (*S*)-**14**, (*R*)-**15**, (*R*)-**16**, (*S*)-**17**, (*R*)-**18**, and (*S*)-**19** exhibited marked, concentration-dependent changes in specific rotation in $CHCl_3$, as shown in Table 7.

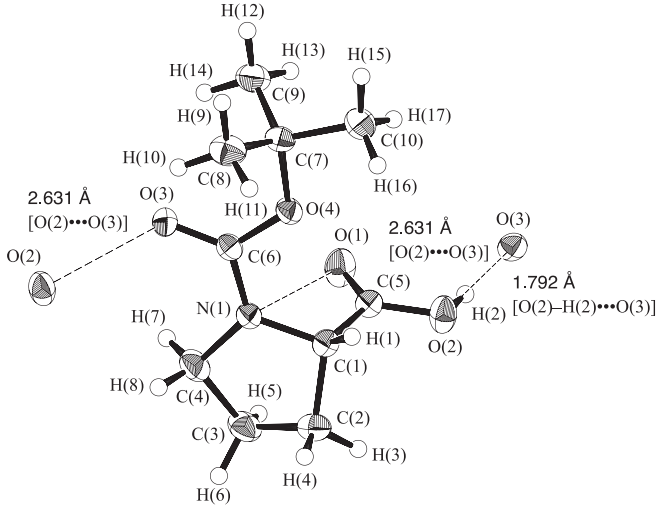


**Fig. 4.** ORTEP drawing of (*S*)-**14**.

### 3.3. *Crystallographic studies of (S)-**13**, (S)-**10**, and (S)-**14***

For compounds (*S*)-**13**, (*S*)-**10**, and (*S*)-**14**, for which good crystals were obtained by recrystallization from the corresponding solvent [$CHCl_3$–*n*-hexane for (*S*)-**13**, $Et_2O$–*n*-hexane for (*S*)-**10**, and $CHCl_3$–*n*-hexane for (*S*)-**14**] at room temperature, intermolecular hydrogen bonding in the solid state were estimated by single crystal X-ray crystallography. In the case of (*S*)-**13**, two kinds of OH···OH intermolecular hydrogen bonds were observed. The distance of O(1)–H(1)···O(2) was 1.971 Å [O(1)···O(2): 2.7896 Å], and the distance of O(2)–H(2)···O(1) was 1.912 Å [O(2)···O(1): 2.7474 Å] (Fig. 2). Two kinds of C = O···HO intermolecular hydrogen bonds, O(3)–H(2)···O(4) and O(1)–H(1)···O(2), were also observed in (*S*)-**10** as shown in Fig. 3. The distance of O(3)–H(2)···O(4) was 1.954 Å [O(3)···O(4): 2.782 Å], and the distance of O(1)–H(1)···O(2) was 1.833 Å [O(1)···O(2): 2.663 Å]. Among these three compounds, the shortest intermolecular hydrogen bond was observed in (*S*)-**14**, in which the C = O···HO-type interaction was between O(2)–H(2) and O(3), and the distance was 1.792 Å [O(2)···O(3): 2.631 Å] (Fig. 4).

### 3.4. *$^1$H NMR analysis of optically active glycerol analogues and structurally related compounds*

The chemical shift of $^1$H NMR spectroscopy is a powerful tool for probing of intermolecular hydrogen bonding, and thus the $^1$H NMR spectra of (*S*)-**1**, (*S*)-**6**, (*S*)-**13**, and (*R*)-**8a** were measured at different concentrations, as shown in Table 8. From the $^1$H NMR spectrum of (*S*)-**1** in $CDCl_3$, both hydrogen atoms $H_A$ and $H_B$ of the hydroxy groups were observed at about 1 ppm lower magnetic field at high concentration (85 mg/0.6 mL) than at low concentration (6 mg/0.6 mL). The chemical shifts of hydrogen atoms $H_C$ were observed at slightly higher magnetic fields at high concentration in $CDCl_3$, but no concentration-dependent changes were observed in $CD_3OD$.

$^1$H NMR spectra of (*S*)-**11** and (*S*)-**14** were also measured at different concentrations in $CDCl_3$ as shown in Table 9. The chemical shifts of hydrogen atoms $H_A$ of the hydroxy and carboxy groups were observed in a concentration-dependent manner at low fields under high concentration conditions, while the chemical shift of the hydrogen atom $H_B$ of the C-H bond showed no concentration-dependent change..

## 4. Conclusions

Specific rotation of optically active glycerol analogues (*S*)-**1**, (*S*)-**6**, and (*S*)-**13** changed its sign from (+) to (–) with increasing concentration in $CHCl_3$. The $^1$H NMR spectrum of (*S*)-**6** showed concentration-dependent changes of chemical shift in $CDCl_3$. In the case of (*S*)-**13**, intermolecular hydrogen bonding was observed by single crystal X-ray crystallography. Based on chemical structural similarity to these glycerol analogues, we found several compounds that exhibit concentration-dependent changes in specific rotation, namely (*S*)-**14**, (*R*)-**15**, (*R*)-**16**, (*S*)-**17**, (*R*)-**18**, and (*S*)-**19**. This series of compounds have multiple functional groups capable of serving as a hydrogen-bond donor and/or acceptor, and the concentration-dependent changes of specific rotation may be due to self-assembly of these compounds via intermolecular hydrogen bonding at high concentration. Therefore, in the measurement of specific rotation of optically active compounds with functional groups that can cause intermolecular hydrogen bonding, the concentrations must be matched exactly with the sample being compared.

**Table 8**
Selected chemical shifts of (*S*)-**1**, (*S*)-**6**, (*S*)-**13**, and (*R*)-**8a** in $^1$H NMR (500 MHz, $CDCl_3$) analysis

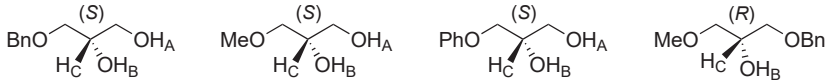


(*S*)-**1** (*S*)-**6** (*S*)-**13** (*R*)-**8a**

.

| Solvent | Conc (g/100 mL) | Chemical shifts (ppm) of (*S*)-**1** | | |
|---|---|---|---|---|
| | | δ ($H_A$) | δ ($H_B$) | δ ($H_C$) |
| $CDCl_3$ | 1.0 (6 mg in 0.6 mL) | 2.06 | 2.57 | 3.86–3.92 |
| $CDCl_3$ | 14 (85 mg in 0.6 mL) | 3.00 | 3.34 | 3.82–3.87 |
| $CD_3OD$ | 1.0 (6 mg in 0.6 mL) | — | — | 3.76–3.81 |
| $CD_3OD$ | 14 (85 mg in 0.6 mL) | — | — | 3.76–3.84 |
| Solvent | Conc (g/100 mL) | Chemical shifts (ppm) of (*S*)-**6** | | |
| | | δ ($H_A$) | δ ($H_B$) | δ ($H_C$) |
| $CDCl_3$ | 0.8 (5 mg in 0.6 mL) | 2.11 | 2.59 | 3.84–3.90 |
| $CDCl_3$ | 13 (75 mg in 0.6 mL) | 3.83–3.92 | 4.11 | 3.83–3.92 |
| Solvent | Conc (g/100 mL) | Chemical shifts (ppm) of (*S*)-**13** | | |
| | | δ ($H_A$) | δ ($H_B$) | δ ($H_C$) |
| $CDCl_3$ | 0.8 (5 mg in 0.6 mL) | 2.11 | 2.68 | 4.09–4.14 |
| $CDCl_3$ | 5.0 (30 mg in 0.6 mL) | 3.15 | 3.54 | 4.05–4.11 |
| $CDCl_3$ | 13 (75 mg in 0.6 mL) | 3.85 | 4.15 | 4.01–4.08 |
| Solvent | Conc (g/100 mL) | Chemical shifts (ppm) of (*R*)-**8a** | | |
| | | δ ($H_A$) | δ ($H_B$) | δ ($H_C$) |
| $CDCl_3$ | 0.2 (1.2 mg in 0.6 mL) | — | 2.44 | 3.96–4.02 |
| $CDCl_3$ | 0.8 (5 mg in 0.6 mL) | — | 2.46 | 3.96–4.02 |
| $CDCl_3$ | 13 (75 mg in 0.6 mL) | — | 2.78 | 3.95–4.00 |

**Table 9**
Selected chemical shifts of (*S*)-**11** and (*S*)-**14** in $^1$H NMR (500 MHz, $CDCl_3$) analysis

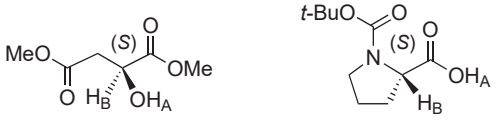


(*S*)-**11** (*S*)-**14**

.

| Solvent | Conc (g/100 mL) | Chemical shifts (ppm) of (*S*)-**11** | |
|---|---|---|---|
| | | δ ($H_A$) | δ ($H_B$) |
| $CDCl_3$ | 0.8 (5 mg in 0.6 mL) | 3.21 | 4.51 |
| $CDCl_3$ | 5.0 (30 mg in 0.6 mL) | 3.33 | 4.52 |
| $CDCl_3$ | 13 (75 mg in 0.6 mL) | 3.47 | 4.53 |
| Solvent | Conc (g/100 mL) | Chemical shifts (ppm) of (*S*)-**14** | |
| | | δ ($H_A$) | δ ($H_B$) |
| $CDCl_3$ | 0.8 (5 mg in 0.6 mL) | — [a)] | 4.22–4.39 |
| $CDCl_3$ | 5.0 (30 mg in 0.6 mL) | 10.7 | 4.21–4.40 |
| $CDCl_3$ | 13 (75 mg in 0.6 mL) | 11.3 | 4.21–4.40 |

a) Broad signal.

## CRediT authorship contribution statement

**Michiyasu Nakao:** Data curation, Investigation, Validation, Writing – review & editing. **Akihito Nakamura:** Investigation, Validation. **Shoki Yamada:** Validation. **Syuji Kitaike:** Investigation. **Shigeki Sano:** Conceptualization, Data curation, Project administration, Supervision, Writing – original draft, Writing – review & editing.

## Declaration of competing interest

The authors declare that they have no known competing financial interests or personal relationships that could have appeared to influence the work reported in this paper.

## Data availability

No data was used for the research described in the article.

## Appendix A. Supplementary data

Supplementary data to this article can be found online at https://doi.org/10.1016/j.rechem.2024.101415.

## References


[1] B. Testa, J. Caldwell, M.V. Kisakürek, Organic stereochemistry: guiding principles and biomedicinal relevance, Wiley-VCH Verlag GmbH, Ochsenfurt, 2012, pp. 206–209.
[2] J. Clayden, N. Greeves, S. Warren, Organic chemistry, second ed., Oxford University Press, Silisbury, 2018, pp. 309–310.
[3] P. Vollhardt, N. Schore, Organic chemistry: structure and function, eighth ed., W.H. Freeman and Company, New York, 2018, pp. 187–190.
[4] D.R. Klein, Organic chemistry, fourth ed.,, John Wiley & Sons Singapore Pte. Ltd., 2021, pp. 200–205.
[5] J.M. Karty, Organic chemistry: principles and mechanisms, third ed., W. W. Norton & Company, New York, 2022, pp. 245–248.
[6] S. Sano, H. Sumiyoshi, A. Handa, R. Tokizane, M. Nakao, Tetrahedron Lett. 56 (2015) 4686–4688.
[7] M. Nakao, K. Tanaka, S. Kitaike, S. Sano, Synthesis 49 (2017) 3654–3661.
[8] M. Brard, C. Lainé, G. Réthoré, I. Laurent, C. Neveu, L. Lemiègre, T. Benvegnu, J. Org. Chem. 72 (2007) 8267–8279.
[9] A.M. Thompson, H.S. Sutherland, B.D. Palmer, I. Kmentova, A. Blaser, S. G. Franzblau, B. Wan, Y. Wang, Z. Ma, W.A. Denny, J. Med. Chem. 54 (2011) 6563–6585.
[10] K. Toribatake, H. Nishiyama, Angew. Chem. Int. Ed. 52 (2013) 11011–11015.
[11] B. Kristinsson, K.M. Linderborg, H. Kallio, G.G. Haraldsson, Tetrahedron: Asymmetry 25 (2014) 125–132.
[12] T. Tsujigami, T. Sugai, H. Ohta, Tetrahedron: Asymmetry 12 (2001) 2543–2549.
[13] G. Sabitha, G.S.K.K. Reddy, K.B. Reddy, N.M. Reddy, J.S. Yadav, J. Mol. Catal. A Chem. 238 (2005) 229–232.
[14] T.M. Shaikh, A. Sudalai, Tetrahedron: Asymmetry 20 (2009) 2287–2292.
[15] J.M. Park, K.A. De Castro, H. Ahn, H. Rhee, Bull. Korean Chem. Soc. 31 (2010) 2689–2691.
[16] R.T. Sawant, S.B. Waghmode, Tetrahedron 66 (2010) 2010–2014.
[17] S. Casati, P. Ciuffreda, E. Santaniello, Tetrahedron: Asymmetry 22 (2011) 658–661.
[18] H.D. Dakin, J. Biol. Chem. 59 (1924) 7–12.
[19] W.D. Bancroft, H.L. Davis, J. Phys. Chem. 34 (1930) 897–928.
[20] A. Altomare, M.C. Burla, M. Camalli, G.L. Cascarano, C. Giacovazzo, A. Guagliardi, A.G.G. Moliterni, G. Polidori, R. Spagna, J. Appl. Cryst. 32 (1999) 115–119.
[21] CrystalStructure 4.0: Crystal Structure Analysis Package, Rigaku Corporation (2000-2010). Tokyo 196–8666, Japan.
[22] S. Nakamura, M. Sayama, A. Uwamizu, S. Jung, M. Ikubo, Y. Otani, K. Kano, J. Omi, A. Inoue, J. Aoki, T. Ohwada, J. Med. Chem. 63 (2020) 9990–10029.
[23] D.E. White, P.M. Tadross, Z. Lu, E.N. Jacobsen, Tetrahedron 70 (2014) 4165–4180.
[24] H. Hattori, T. Mitsunaga, D.L.J. Clive, Tetrahedron Lett. 60 (2019) 1989–1991.
[25] L. Börjesson, C.J. Welch, Tetrahedron 48 (1992) 6325–6334.
[26] I. Izquierdo, M.T. Plaza, R. Robles, A. Mota, Tetrahedron: Asymmetry 8 (1997) 2597–2606.
[27] P.I. Nagy, Int. J. Mol. Sci. 15 (2014) 19562–19633.